

# Enhanced CT simulation using realistic vascular flow dynamics

Cyrus Tanade<sup>1\*</sup>, Nicholas Felice<sup>2\*</sup>, Ehsan Abadi<sup>2</sup>, Ehsan Samei<sup>2</sup>, Amanda Randles<sup>1</sup>, and W. Paul Segars<sup>2</sup>

<sup>1</sup>Dept. of Biomedical Engineering, Duke University, Durham, NC, USA; <sup>2</sup>Carl E. Ravin Advanced Imaging Laboratory, Dept. of Radiology, Duke University, Durham, NC, USA

\*These authors contributed equally to the work

## ABSTRACT

As medical technologies advance with increasing speed, virtual imaging trials (VITs) are emerging as a crucial tool in the evaluation and optimization of new imaging techniques. Widely used in many VITs is the four-dimensional extended cardiac-torso (XCAT) phantom, a comprehensive computational model that accurately represents human anatomy and physiology. While the XCAT phantom offers a powerful tool for imaging research, it offers only a limited model of blood flow to compartmentalized organs, potentially limiting the realism and clinical applicability of contrast-enhanced scan simulations. This study bridges that gap by combining realistic CT simulation with an accurate model of blood flow dynamics to enable more realistic simulations of contrast-enhanced imaging. To achieve this, a validated one-dimensional blood flow simulator, HARVEY<sub>1D</sub>, was used to model flow throughout the vessels of the XCAT phantom. DukeSim, a validated CT simulation platform, was then modified to incorporate the resulting flow into its simulations, thus enabling the generation of simulated CT scans reflective of real-world blood-based contrast-enhanced imaging scenarios. To demonstrate the utility of this pipeline in an initial application to cardiac imaging, three heart models were studied: a non-diseased model, a 50% stenosis model, and an 80% stenosis model. Three seconds of contrast propagation were tracked in each heart model, and CT scans corresponding to two timepoints were simulated. Results demonstrated that the presence of stenosis significantly impacted blood flow, with greater resistance to blood flow leading to altered flow patterns visible in the simulated CT images. This work showcases a pipeline that leverages both computational fluid dynamics and medical imaging simulations to enhance the realism of virtual imaging trials and facilitate the evaluation, optimization, and development of diagnostic tools for contrast-enhanced imaging.

**Keywords:** Simulation, virtual trials, computed tomography, contrast-enhanced imaging

## 1. INTRODUCTION

The four-dimensional extended cardiac-torso (XCAT) phantom is a vital tool widely used in medical imaging research to evaluate and improve upon existing imaging techniques [1]. The XCAT phantom is a computational model of human anatomy and physiology that accurately models a range of patient attributes, including variations in body size, anatomical structures, and patient motion [2]. By interfacing this phantom with a computerized imaging system model, simulated medical images reflecting various imaging scenarios can be generated [3]. One tool for performing such simulations is DukeSim, a validated, scanner-specific CT simulation platform [4]. However, neither the XCAT phantom nor DukeSim account for contrast propagation within blood vessels.

The objective of this work is to combine accurate blood flow modeling from HARVEY<sub>1D</sub> with realistic CT simulation to enable more realistic simulations of contrast-enhanced imaging. We performed an initial demonstration of the enhanced virtual trial pipeline in cardiac imaging by modeling flow for three cases of increasing stenosis in the coronary arteries. Coronary CT angiography (CCTA) is an increasingly popular diagnostic tool for patients showing symptoms of coronary artery disease. The development of techniques to quantify and characterize plaques through CCTA is an active area of research, and one in which such realistic virtual imaging trials have the potential to facilitate further advancements.

## 2. METHODS

A standard adult male XCAT phantom, 50<sup>th</sup> percentile in height and weight, was used as the virtual patient in the simulations. The unmodified phantom provided the healthy case ( $S_0$ ). The phantom was modified by placing blocks in the left and right coronary arteries resulting in a 50% stenosis case ( $S_1$ ) and an 80% stenosis case ( $S_2$ ).

We used our high-resolution 1D blood flow simulator, HARVEY<sub>1D</sub> [5], [6], to model flow. As 1D models only resolve flow in the longitudinal direction of flow, contrast is assumed to be constant over cross-sections. The 1D model is based on the Navier-Stokes equations. 1D geometries were obtained by extracting centerlines of 3D segmented geometries using Mimics (Materialise, Belgium). To model contrast agent transport, we coupled a two-phase flow model to the 1D blood simulator as done in [5]. At each timestep, once the full flow field is computed, the coupled flow model solves 1D transport equations [7] that advect volume fractions of contrast. To accurately model the effects of stenoses, we coupled the 1D model to an empirically-derived pressure-loss equation that has been validated for coronaries [6], [8].

Blood was modeled as an incompressible Newtonian fluid with a density of 1060 kg/m<sup>3</sup> and dynamic viscosity was assumed to be 4 cP. We used steady flowrate boundary conditions at the inlet and 2-element Windkessel models at the outlets. Outlet conditions were tuned to the geometry using Murray's Law [9]. To model the effects of stenoses on contrast agent propagation, we performed modifications to our baseline and non-disease geometry ( $S_0$ ). As mentioned above,  $S_1$  includes 50% stenoses in the right and left coronary arteries.  $S_2$  is a more severe case with 80% stenoses in the right and left coronaries. We applied the same blood flow properties and boundary conditions to the three geometries. Blood flow was resolved for 3 seconds. The contrast agent was injected with a volume fraction of 1 for the first second of the simulation. The results of the 1D simulation were voxelized by computing the nearest distance between centerline coordinates and 3D voxel coordinates. As there were millions of voxels, we applied a K-D tree, which is a space-partitioning data structure, to perform the nearest distance computations efficiently.

From the contrast flow simulation, DukeSim takes as input a file that defines the contrast concentration in each lumen-containing voxel. The voxels are sorted into fifty uniformly spaced bins based on their contrast concentrations. For this set of simulations, volume fractions were linearly scaled such that the maximum concentration of contrast targeted 300 Hounsfield units, representing a high level of contrast [10]. For each bin, the elemental composition and density of the corresponding mixture of blood and contrast is calculated. The materials for all organs, including blood, were defined based on material density and elemental compositions defined in the International Commissions for Radiation Units Report 46 [11]. The contrast agent was defined as iopamidol. The elemental composition is used to calculate the mean free paths of photon interactions and linear attenuation coefficient for the material found in each bin. The mean free paths and linear attenuation coefficients are used to generate the scatter and primary signals, respectively.

CT simulations were acquired from all three cases using static snapshots of the heart models at 0.5 seconds and 1.25 seconds of flow simulation to demonstrate the change in contrast enhancement over time due to blood flow. Simulated scans were generated using a scanner-agnostic CT model and reconstructed with vendor-neutral reconstruction software (MCR Toolkit [12]). Mean and standard deviation HU values were taken from ROIs proximal to the stenoses in the right and left coronary arteries at 1.25 seconds to measure the change in contrast flow resulting from different levels of stenosis.

In addition to the static simulations, one CT simulation using real-time contrast flow was acquired from  $S_2$  to demonstrate the time-domain capabilities of HARVEY<sub>1D</sub> and DukeSim. Three seconds of contrast flow was obtained from HARVEY<sub>1D</sub> with a temporal resolution of 10 milliseconds, resulting in 300 timepoints. Heart motion was not modeled. The simulation was acquired as a helical scan with 500 millisecond rotation time, simulating a total scan time of 2.5 seconds.

For every projection, each voxel's linear attenuation coefficient was linearly interpolated from the two nearest timepoints to generate a smooth change in contrast enhancement.

### 3. RESULTS

Figure 1A shows the contrast flow within the XCAT phantoms over time calculated using HARVEY<sub>1D</sub>.  $S_0$  and  $S_1$  have similar contrast flow profiles, which indicates that the 50% stenosis was non-flow limiting.  $S_2$  demonstrated that flow into both coronaries was impeded. Figure 1B are snapshots at 0.5 and 1.25 s of simulation, which were further used to couple with DukeSim. At these two timepoints (Figure 1C), contrast flow in  $S_2$  traverses the descending aorta faster than in  $S_0$  and  $S_1$ . This result indicates that the overall effective resistance to both coronaries is increased with the presence of 80% stenoses, which causes more flow to the aorta and less flow to the coronaries. The same effect is also highlighted in the coronaries, where at 1.25 s, the left coronaries in  $S_0$  and  $S_1$  are almost fully perfused whereas contrast has only begun to reach  $S_2$ .

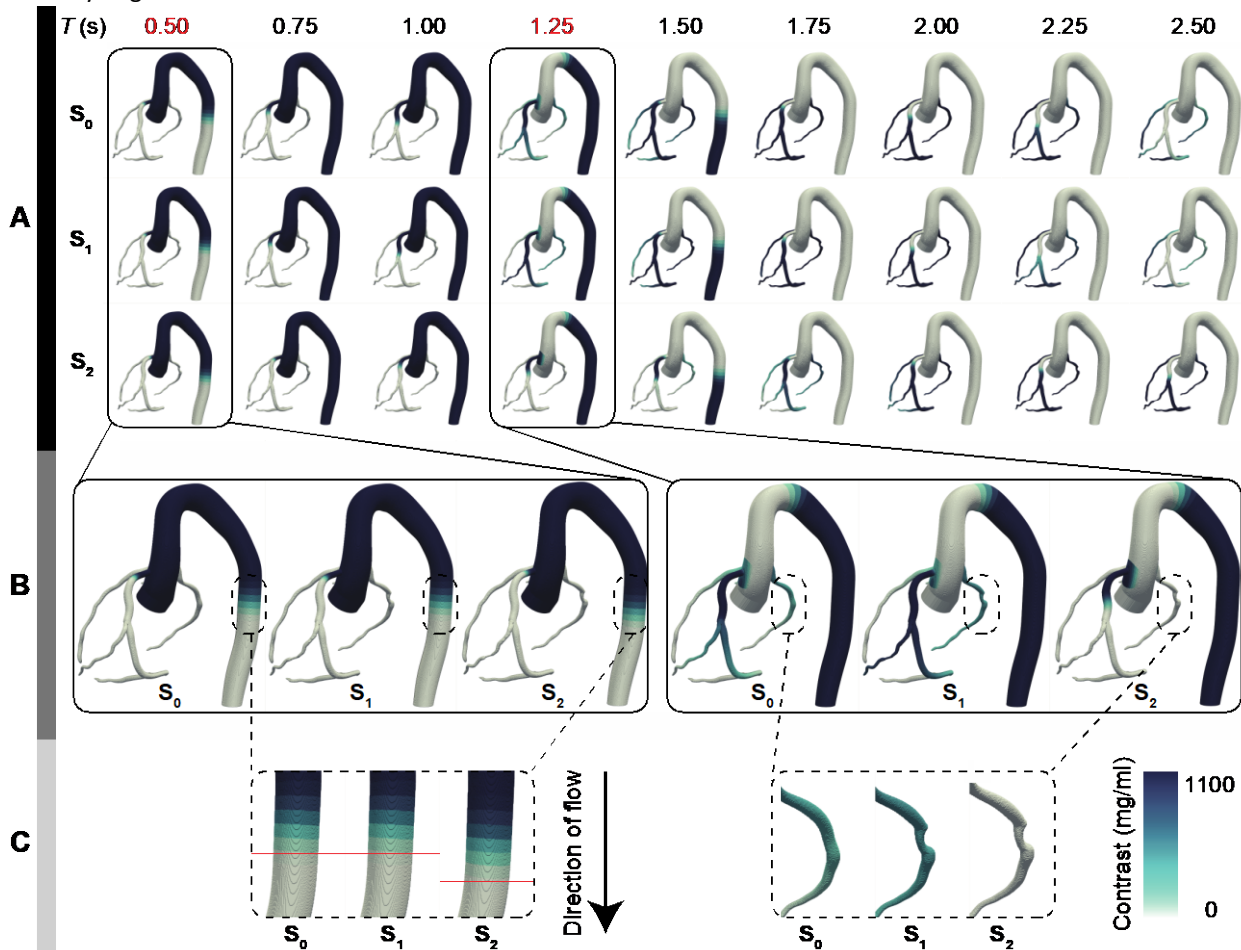


Figure 1: Flow of three models with varying degrees of stenoses.  $S_0$  is an undiseased case,  $S_1$  contains non-flow limiting 50% stenoses in the left and right coronaries, and  $S_2$  contains severe, flow-limiting 80% stenoses in the left and right coronaries. (A) Flow of the models over time (0.50-2.50 s). (B) Models at 0.50 and 1.25 s were used for integration with DukeSim. (C) The flow limiting case,  $S_2$ , demonstrates that contrast propagation is slower with 80% stenoses compared to the other two cases. (Left) Red lines delineate the leading edge of the contrast in the descending aorta.

Figure 2 shows simulated CT scans acquired at 0.5 and 1.25 s of flow simulation. At 1.25 s, the HU values in an ROI within the left coronary are  $146 \pm 33$ ,  $125 \pm 26$ , and  $21 \pm 15$  HU for  $S_0$ ,  $S_1$ , and  $S_2$ , respectively. In the right coronary artery,

the values are  $225\pm 42$ ,  $226\pm 39$ , and  $21\pm 14$  HU for  $S_0$ ,  $S_1$ , and  $S_2$ , respectively. In both cases, the artery is clearly enhanced for  $S_0$  and  $S_1$ , but not  $S_2$ . These results illustrate that the altered flow dynamics caused by stenoses lead to prominent qualitative and quantitative differences in contrast levels throughout the arteries.

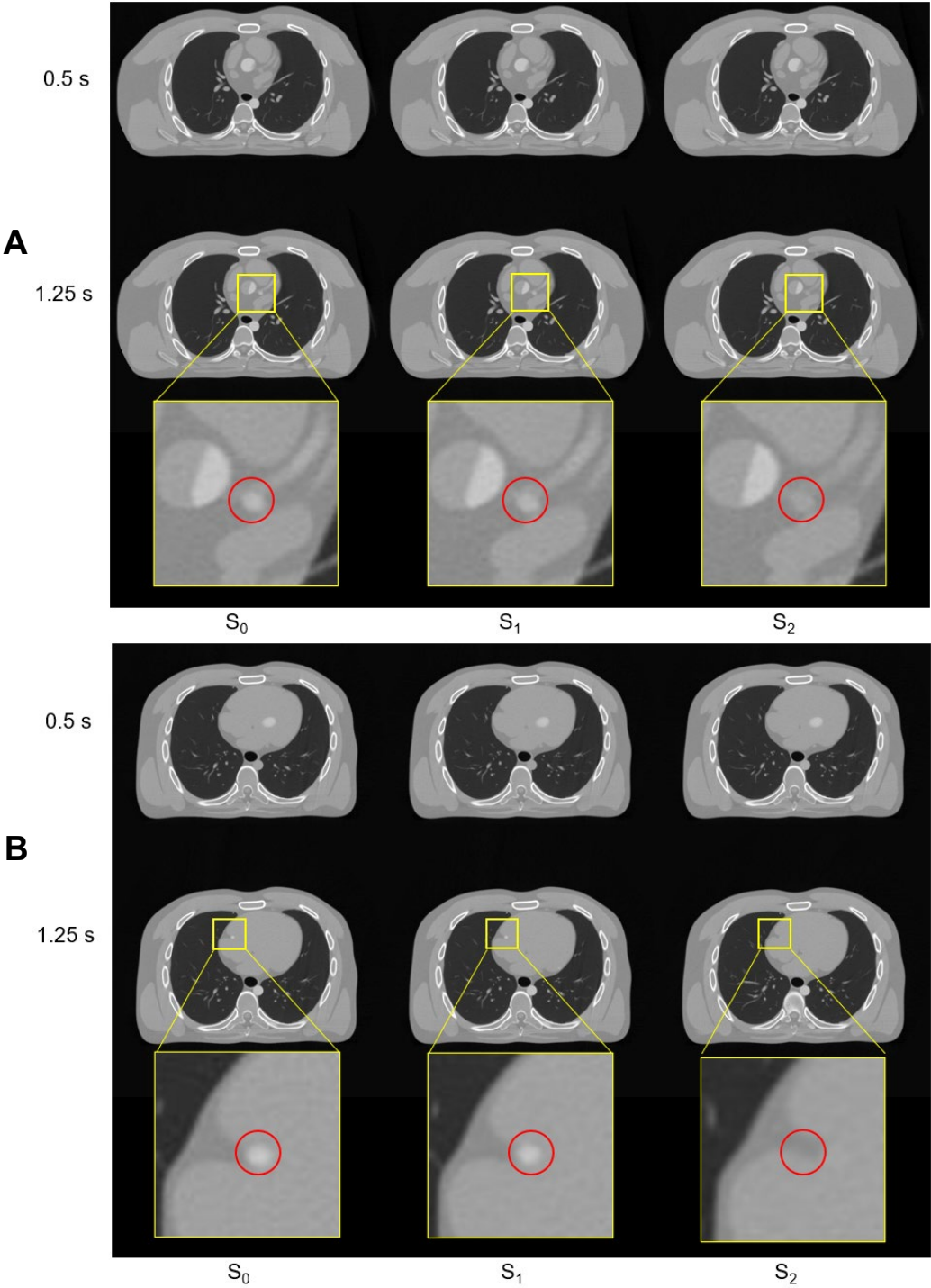


Figure 2: CT simulations of three heart models with varying degrees of stenosis at two timepoints. At 0.5 seconds, contrast flow appears similar across all models. At 1.25 seconds, the decreased blood flow is visible in the coronary arteries (red circles) of the

flow-limiting case ( $S_2$ ) compared to the non-diseased case ( $S_0$ ) and the 50% stenosis case ( $S_1$ ). (A) Slice 24. The bottom row is zoomed in on the left coronary artery. (B) Slice 35. The bottom row is zoomed in on the right coronary artery.

Figure 3 shows a comparison between static and real-time contrast flow CT simulations. Due to the helical acquisition, different slices are acquired at different times. Therefore, the level of contrast enhancement in the aorta changes as a function of slice in the real-time simulation, whereas it is relatively constant in the static simulation.

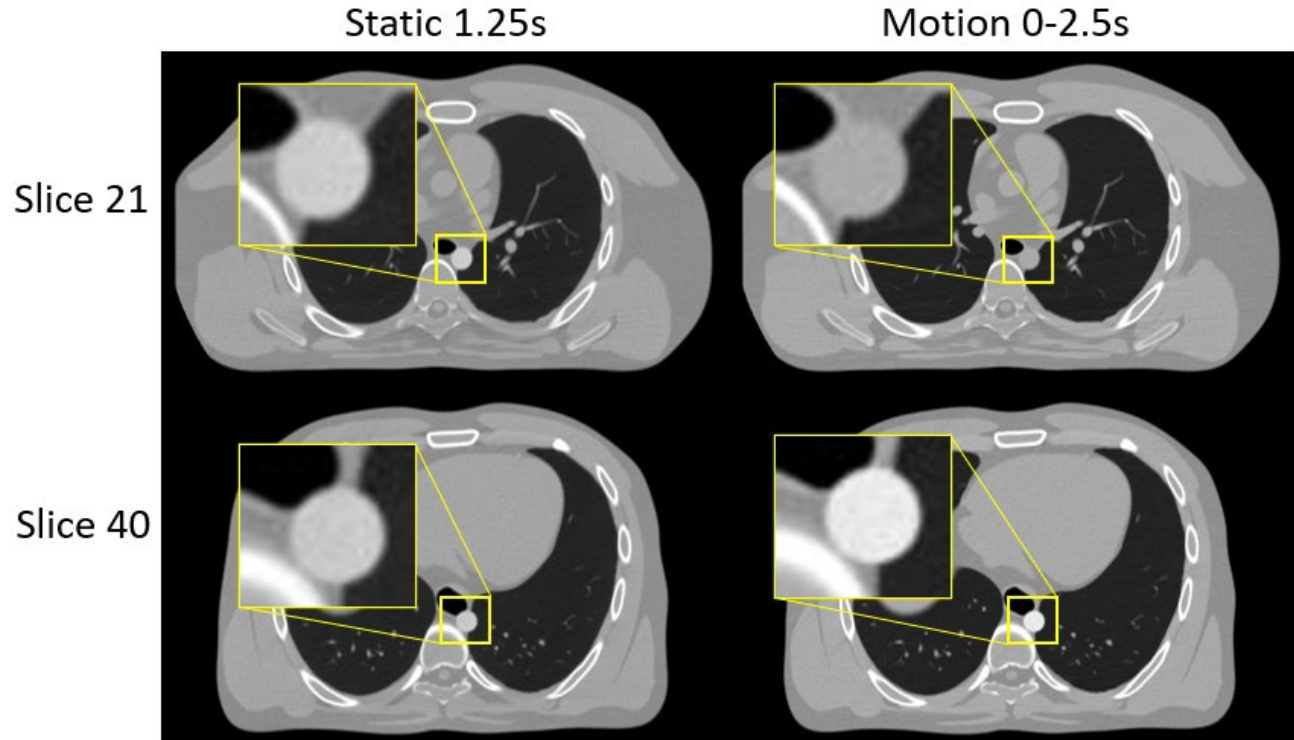


Figure 3: Comparison of static (left) and real-time (right) CT simulations.

## 5. CONCLUSION

Through the use of contrast flow-enhanced simulations, we demonstrated that the severity of stenosis in the coronary arteries has a substantial effect on vessel appearance in CT images. The pipeline we developed introduces a vital tool for future research in contrast-enhanced imaging by accounting for blood flow dynamics in virtual imaging trials.

## REFERENCES

- [1] W. P. Segars, B. M. W. Tsui, C. Jing, Y. Fang-Fang, G. S. K. Fung, and E. Samei, "Application of the 4-D XCAT Phantoms in Biomedical Imaging and Beyond," *IEEE Trans Med Imaging*, vol. 37, no. 3, pp. 680-692, Mar 2018, doi: 10.1109/TMI.2017.2738448.
- [2] W. P. Segars, G. Sturgeon, S. Mendonca, J. Grimes, and B. M. Tsui, "4D XCAT phantom for multimodality imaging research," *Med Phys*, vol. 37, no. 9, pp. 4902-15, Sep 2010, doi: 10.1118/1.3480985.
- [3] E. Abadi *et al.*, "Virtual clinical trials in medical imaging: a review," *J Med Imaging (Bellingham)*, vol. 7, no. 4, p. 042805, Jul 2020, doi: 10.1117/1.JMI.7.4.042805.
- [4] E. Abadi, B. Harrawood, S. Sharma, A. Kapadia, W. P. Segars, and E. Samei, "DukeSim: A Realistic, Rapid, and Scanner-Specific Simulation Framework in Computed Tomography," *IEEE Trans Med Imaging*, vol. 38, no. 6, pp. 1457-1465, Jun 2019, doi: 10.1109/TMI.2018.2886530.

- [5] B. Feiger, A. Kochar, J. Gounley, D. Bonadonna, M. Daneshmand, and A. Randles, "Determining the impacts of venoarterial extracorporeal membrane oxygenation on cerebral oxygenation using a one-dimensional blood flow simulator," *J Biomech*, vol. 104, p. 109707, May 7 2020, doi: 10.1016/j.jbiomech.2020.109707.
- [6] C. Tanade, S. J. Chen, J. A. Leopold, and A. Randles, "Analysis identifying minimal governing parameters for clinically accurate in silico fractional flow reserve," *Front Med Technol*, vol. 4, p. 1034801, 2022, doi: 10.3389/fmedt.2022.1034801.
- [7] W. Aniszewski, T. Ménard, and M. Marek, "Volume of Fluid (VOF) type advection methods in two-phase flow: A comparative study," *Comput. Fluids*, vol. 97, pp. 52-73, Jun. 2014, doi: 10.1016/j.compfluid.2014.03.027.
- [8] C. Tanade, B. Feiger, M. Vardhan, S. J. Chen, J. A. Leopold, and A. Randles, "Global Sensitivity Analysis For Clinically Validated 1D Models of Fractional Flow Reserve," *Annu Int Conf IEEE Eng Med Biol Soc*, vol. 2021, pp. 4395-4398, Nov 2021, doi: 10.1109/EMBC46164.2021.9629890.
- [9] T. F. Sherman, "On connecting large vessels to small. The meaning of Murray's law," *J Gen Physiol*, vol. 78, no. 4, pp. 431-53, Oct 1981, doi: 10.1085/jgp.78.4.431.
- [10] L. La Grutta *et al.*, "Comparison of iodinated contrast media for the assessment of atherosclerotic plaque attenuation values by CT coronary angiography: observations in an ex vivo model," *Br J Radiol*, vol. 86, no. 1021, p. 20120238, Jan 2013, doi: 10.1259/bjr.20120238.
- [11] U. International Commission on Radiation and Measurements, *Photon, electron, proton, and neutron interaction data for body tissues* (ICRU report 46). Bethesda, Md., U.S.A: International Commission on Radiation Units and Measurements (in English), 1992, pp. vii, 207 p. : ill.
- [12] D. Clark and C. Badea, "MCR Toolkit: A GPU-based toolkit for Multi-Channel Reconstruction of preclinical and clinical X-ray CT data," *Med Phys*, 2023.